ISSN 0027-1349, Moscow University Physics Bulletin, 2016, Vol. 71, No. 6, pp. 527–536. © Allerton Press, Inc., 2016.
Original Russian Text © E.A. Kulikov, V.K. Gusiakov, A.A. Ivanova, B.V. Baranov, 2016, published in Vestnik Moskovskogo Universiteta, Seriya 3: Fizika, Astronomiya, 2016, No. 5, pp. 14–32.

PHYSICS OF EARTH, ATMOSPHERE, AND HYDROSPHERE (REVIEW)

Numerical Tsunami Modeling and the Bottom Relief

E. A. Kulikov[a]*, V. K. Gusiakov[b, c], A. A. Ivanova[a], and B. V. Baranov[a]

[a] *Shirshov Institute of Oceanology, Russian Academy of Sciences, Nakhimovskii pr. 36, Moscow, 117997 Russia*

[b] *Institute of Computational Technologies, Siberian Branch, Russian Academy of Sciences, pr. Akademika Lavrent'eva 6, Novosibirsk, 630090 Russia*

[c] *Institute of Computational Mathematics and Mathematical Geophysics, Siberian Branch, Russian Academy of Sciences, pr. Akademika Lavrent'eva 6, Novosibirsk, 630090 Russia*

**e-mail: kulikove@ocean.ru*

Received May 31, 2016; in final form, June 24, 2016

Abstract—The effect of the quality of bathymetric data on the accuracy of tsunami-wave field calculation is considered. A review of the history of the numerical tsunami modeling development is presented. Particular emphasis is made on the World Ocean bottom models. It is shown that the modern digital bathymetry maps, for example, GEBCO, do not adequately simulate the sea bottom in numerical models of wave propagation, leading to considerable errors in estimating the maximum tsunami run-ups on the coast.

Keywords: tsunami, numerical model, bottom relief, bathymetric data.

DOI: 10.3103/S002713491605012X

INTRODUCTION

Development of methods for early tsunami warning and obtaining long-term tsunami-hazard assessments is largely based on computer modeling. In early tsunami warning, numerical models are necessary for early estimation of the expected tsunami height on the coast from seismological observations and calculated earthquake-source parameters. In the problems of long-term prediction (tsunami zoning of the coast), computer modeling is used in scenario calculations to obtain the expected heights of tsunamis produced by earthquakes of different magnitudes.

The modern systems for instrumental tsunami monitoring (for example, the DART system of submarine buoys [1]) can detect tsunami signals early and at a significant distance from the coast. However, calculation of the arrival time and tsunami height for the particular shore site requires the use of effective computational methods of tsunami propagation in the deep ocean and on the shelf.

Another important problem is tsunami zoning of the coasts (i.e., preliminary long-term tsunami-hazard assessment for particular coastal sites). The modern approach to solution of this problem is based on the Probabilistic Tsunami-Hazard Assessment (PTHA) technique [2], which utilizes the results of numerical simulation of tsunami propagation from the model sources located in the main seismoactive (tsunamigenic) zones in the World Ocean.

The effectiveness of the application of numerical models to solve these main theoretical and practical tsunami problems depends not only on the correctness of the used physical–mathematical models and the respective numerical algorithms, but also on a number of other factors, including the accuracy and degree of detail of the bathymetric data used for the construction of the computational grids.

The present study provides the results of analysis of the effect of bathymetric data quality on the accuracy of tsunami wave field calculation.

1. NUMERICAL MODELING OF TSUNAMI GENERATION AND PROPAGATION

The most widely used *physical* model of a tsunami is the model of so-called *long waves* that propagate in a layer of a homogeneous incompressible liquid above a rigid bottom. Since the wavelengths of typical seismogenic tsunamis generated by submarine earthquake sources in seas and oceans are much longer than depths of water basins, *mathematical* description of tsunami propagation can involve the *shallow-water* approximation where vertical accelerations are neglected and therefore the vertical velocities of particles in the liquid. In this respect, the use of the hydrostatic approximation allows the dependence of horizontal current velocities on the depth to be excluded from 3D equations of motion; as a result, we can proceed to vertically-integrated 2D equations, for example, those relative to level and full flows [3, 4]. This procedure considerably simplifies the modeling of tsunami propagation in ocean compared to the use of full 3D models of Navier–Stokes type.

Numerical methods for calculation of tsunami propagation in particular sites of the ocean area began to be used in the mid-1960s when sufficiently powerful computers (such as IBM-360, CDC-6400, and BESM-6) that were able to perform these calculations became available in computational centers. A detailed analysis of the initial stage of tsunami numerical modeling can be found in [5, 6]. Chronologically, the first publications on the problem appeared in Japan: these were attempts to simulate the tsunami in the Tokyo Bay caused by the 1960 Great Chilean earthquake [7] and to reproduce the main peculiarities of this tsunami propagation across the Pacific Ocean [8]. These studies used a program code that was developed for the modeling of tidal waves and implemented the numerical solution of a nonlinear shallow-water system for a revolving sphere. Calculations of the 1960 Chilean tsunami propagation across the Pacific were made using the IBM-704 first-generation electronic tube machine on a bathymetric grid of 25 × 30 nodes with a spatial step of five degrees (approximately 550 km). The first publication of this kind, which started the evolution of computer models developed exclusively for reproducing the historical cases of tsunamis, was probably the work by I. Aida [9]. The purpose of that study was an attempt to reproduce the main peculiarities of two tsunamis: one in the Sea of Japan caused by the Niigata earthquake of June 16, 1964 and another caused by the Tokachi-Oki earthquake that occurred off the coast of Hokkaido Island on June 16, 1968. Aida's model utilized the finite-difference scheme that approximates shallow-water equations, without the Coriolis force and bottom friction being taken into account, and was written in the rectangular coordinate system. Modeling of the tsunami after the 1964 Niigata earthquake used the data of repeated bathymetric surveys, which was conducted in the source zone immediately after the earthquake and revealed considerable postseismic bottom deformations [10, 11], to set the initial free surface elevation. Thus, Aida's model assumed that bottom displacement occurred instantly and the shape of the initial elevation in the sea surface was the same as that of the bottom elevation. Further evolution of this elevation was determined numerically, with the real shoreline configuration and bottom relief being taken into consideration. Calculation was made on a grid of 20 × 30 nodes with a spatial step of 10 km. Depths in the nodes were set by manual digitization of nautical charts. The calculated distribution of run-ups along the shoreline was compared to the measured run-ups and satisfactory agreement was established between the maximum values and the character of decrease in run-up heights with distance off the source zone.

The analogous approach was used for modeling the tsunami caused by the 1968 Tokachi-Oki earthquake. A grid of 30 × 25 nodes with a 20-km spatial step was used in the calculations. For this tsunami, the character of bottom displacements was known only in the very general form; however, a large number of records from coastal tide gauges were available. Several versions of bottom displacement were considered: these were set quite arbitrarily within the elliptical source zone, whose size and position, in turn, were chosen on the basis of the aftershock data and the calculation results of inverse refraction diagrams [12]. The model of bottom deformation was then chosen by comparison between the calculated and the observed tidal curves to provide the best match with the observed data.

In the United States, the first work on numerical modeling of tsunamis was the paper [13] where the numerical model of the tsunami caused by the Great Alaska earthquake (March 28, 1964) was constructed and propagation of this tsunami in the NE Pacific was modeled. In this work, the authors applied the first-order nonlinear system of motion equations in shallow-water approximation. These equations were transformed into finite-difference form and solved numerically on a grid with a step of approximately 0.5° that covered the source zone and the adjacent water areas. The wave profiles were calculated for several points near the source, but their matching with the real data was not verified because the records of this tsunami from the deep-water part were absent. The water-level variations calculated for one point on the coast were compared to the respective observed data and satisfactory agreement between them was found. In a subsequent publication [14], the model was improved by introducing corrections to the Earth's surface curvature and by writing the main equations in spherical coordinates. This model was later used for modeling the tsunamis from the strongest earthquakes, including the 1960 Great Chilean earthquake, for which displacement characters were more or less reliably known.

The first Russian works on numerical modeling of tsunamis were made at the Siberian Branch of the Russian Academy of Sciences. They investigated the behavior of hypothetical and real historical tsunamis in the region of the South Kuril Islands [15–17] in terms of a nonlinear shallow-water system written in Cartesian coordinates and with a piston model of tsunami generation being assumed.

The very first attempts at the application of numerical methods for modeling real tsunamis showed this to be a very promising approach. Later, a large number of software packages and complexes for tsunami modeling was developed; they were based on more complex models including the effects of the Earth's revolution, amplitude and frequency dispersion, and bottom friction. By the early 1990s the international scientific community on tsunamis reached the conclusion that all the numerical models and software packages for tsunami calculations needed to be verified and validated. In this respect, two special workshops were carried out in the United States; resulting from these workshops, a system for testing the tsunami calculation software was developed and adopted [18, 19].

During the first 2 decades (the 1960s and 1970s), the wide use of computer models for studying tsunamis was limited by the lack of random-access memory

and speeds of the available computers, on the one hand, and by the lack of information about the structure of tsunami sources. The data on coseismic bottom displacements in the source zone, which were obtained by repeated bathymetric measurements, were available only for a few tsunamigenic earthquakes. To estimate the source positions and sizes, the method of inverse refraction diagrams was used; the initial value of the ocean surface displacement was estimated by correlation formulas that approximately linked earthquake magnitude and tsunami height. However, starting from the mid-1970s, systematic data on focal mechanisms of strong earthquakes defined by the CMT (Centroid Moment Tensor) method [20] began to appear. Since 1976, determinations of earthquake focal mechanisms became regular for all earthquakes with Mw = 5.5. [21]. This provided the opportunity to utilize the obtained focal mechanism solutions of the submarine tsunamigenic earthquakes for calculations of residual bottom displacements in the source zone.

The first and, in a certain sense, remarkable work of this kind was another publication by I. Aida [22] where he considered the validity of data on the tsunami source inferred from the data on the focal mechanism of a submarine earthquake. Aida constructed the computer models for five tsunamis that occurred in 1952–69 on the eastern coasts of Honshu and Hokkaido islands after the respective earthquakes, viz., Tokachi-Oki (March 4, 1952 and May 16, 1968), Ivate-Oki (June 12, 1968), Shikotan (August 12, 1969), and Nemuro-Oki (June 17, 1973), for which the data on the orientations and size of the rupture plane and on the slip value were available. Residual bottom displacements in the source zone were calculated on the basis of the formulas obtained in [23]. Displacements were used as initial conditions in the problem of tsunami generation. Further evolution of the initial water elevation was calculated on the basis of the shallow-water linear model solved numerically on the series of embedded grids with spatial steps varying from 10 km in deep-water areas to 312.5 m in the vicinity of tide-gauge observation points in the coastal zone. The comparison between the calculated and measured amplitudes was made only for the head (primary) wave because it was supposed that the following waves could contain considerable computational errors due to insufficient approximation accuracy of coastal bathymetry and the shoreline configuration. The precision of the reproduction for the first wave amplitude calculation appeared to be 50 to 100%, which was quite a good result at that time; calculated arrival times fitted the observed ones within the accuracy of 5–10 min. For every source model, the so-called correction factor K was introduced to show the average (at 4–6 tide-gauge observation points) ratio between the observed and calculated amplitudes. For the majority of the considered source models, this factor appeared to be more than 1, with the average value of 1.4 and total variation range being 0.82–4.45 (i.e., the calculated amplitudes were less than the observed ones, on average). The general conclusion of this work was that in the presence of data on the focal mechanism and with the available instrumentally measured value of the seismic moment of an earthquake, the calculated bottom displacements in the source zone could be used for the construction of quite realistic numerical models of historical tsunamis.

After this, the use of calculated bottom displacements in the source zone as an approximation of the tsunami source (the so-called piston model of tsunami generation) became the standard scheme for the construction of computer models for both historical and hypothetical tsunamis. These displacements were usually calculated by formulas developed by Y. Okada [24]. These formulas represent the static (residual) displacements in the surface of the homogeneous elastic half-space, which occur under the effect of the internal spatial source of the dislocation type; in turn, the source is set by six parameters: the length and width of the rupture plane, the dipping angle of this plane, slip direction, striking azimuth, depth of the upper (or lower) rupture edge, and slip value (dislocation length). In fairness, it must be noted that the mentioned work by Y. Okada [24] was only the final one in a series of publications devoted to the solution of this problem. In terms of different approaches to the problem statement and solution methods, this problem was considered in [25–29]. In Russia, formulas analogous to those derived in [24] were obtained in [30]. At a certain difference between the forms of the final expressions for displacement components, multiple tests showed the absolute identity of the final results obtained by both sets of formulas at any set parameters of the model sources.

Until the early 2000s, the uniform slip along the rupture plane that simulated the earthquake source was used as the model of a tsunami source; displacements from this slip were calculated by formulas obtained by Y. Okada [24], in this case. Evolution of seismic observation systems towards the use of broadband digital instruments, jointly with the application of methods from the theory of inverse problem for the restoration of the fine structure of the source allowed the researchers to use the data on the real slip distribution on the rupture plane [31]; Okada's formulas are applied for each fragment (plane) of the slip distribution, into which one or several rupture planes are subdivided in the source of a real earthquake. This technique is currently used in the majority of works dealing with numerical simulation of the real historical tsunamis (see the reviews, for example, in [4, 32, 33]) that analyze the properties of coseismic deformations in tsunami sources [34–36].

The quality of numerical modeling of tsunami generation and propagation is at very good level today. Deep-water tsunami records obtained by DART sensors [37] are usually reproduced in calculations within very good accuracy (5–10%) in defining the first wave

amplitude [38, 39]. The instrumental records of the head tsunami wave that are obtained in particular bays (especially those located in the far zone of the source), are usually not difficult to reproduce through calculations (even in the case of online calculations) [40].

However, an adequate reproduction of tsunamis in records of tide gauges and modeling of run-ups in the near zone of the source are still problematic, even when the synthetic tide-gauge records reproduce the records of real deep-water sensors well. It is natural that modeling of both tsunami propagation in shallow water and tsunami run-up on shore is a much more complex problem to solve compared to the modeling of wave propagation in deep water. In this case, the amplitude dispersion must be taken into account, but it is possible only in terms of a nonlinear system, with bottom friction taken into consideration, and by applying special numerical methods for modeling the wave run-up onto a dry shore. The modern models of run-up usually take all these factors into consideration, but the problems of precise reproduction of water-level variations in shallow water and adequate calculation of the maximum run-up remain.

The significant difference between calculated and measured tsunami heights (not even tens, but hundreds of percent) can be related to the above-mentioned problems of tsunami source setting, the effectiveness of the numerical algorithm, and the detail of the grid, on the one hand, but also the accuracy of the approximation to the real sea-bottom bathymetry. The present work is devoted to estimation of the quality of the contemporary bathymetric maps of the World Ocean and to assessment of possible errors that emerge when numerical simulation of tsunamis due to inadequateness of the used bathymetric data.

2. DATA ON THE BATHYMETRY OF THE WORLD OCEAN

In the early works on tsunami modeling in the 1960s and 1970s, grid massifs were usually made by researchers themselves by manual digitization of marine nautical charts [10]. The first widely accessible massif of global bathymetric data was ETOPO5, which was formed in 1988 and contained land altitudes and sea depths rounded to meters on the grid with a resolution of five angular minutes. The massif was developed in the United States by integration of topographic and bathymetric data from various sources. The real accuracy of depth values varies from a few to 100–150 meters in the water areas that are weakly covered by marine surveys [41].

The international GEBCO (General Bathymetric Chart of Oceans) program, which has been supported by the International Hydrological Organization (IHO) since 1903 released the first digital version of the GEBCO atlas in 1994 [42]. The digital version was based on the fifth edition of the traditional GEBCO atlas, which was published in 1978 and showed the World Ocean bathymetry in the form of isolines and particular point measurements; in fact, the digital version was a scanned copy of the GEBCO bathymetric contour maps.

Another important stage was the development of the global gridded data sets of elevations and depths with a spatial resolution of two angular minutes [43]. The data source was high-precision satellite measurements of the land elevations and the ocean free surface; then, the recorded gravity anomalies were recalculated by a quite complex algorithm into a function that describes the bottom relief. This algorithm works well for abyssal depths of more than 1 kilometer, whereas it yields high (sometimes up to 50–100%) relative errors in depth estimation for shallow-water areas (marginal seas, continental slope, and continental shelf). These errors are mainly caused by uncertainties in the determination of the thickness of the loose sediments on the bottom.

The GEBCO gridded bathymetric data set with resolution of one angular minute (GEBCO_08) was published in 2008. Depths in nodes of the regular grid were calculated by interpolation of digitized isobaths and point measurements from the GEBCO digital atlas that was issued on the 100th anniversary of the project [44].

In March 2015, the GEBCO_2014 gridded bathymetric data set was released. It contained land altitudes and sea depths with a resolution of 30 angular seconds. This data set was compiled on the basis of a large number of sources: national and regional organizations (NOAA, European Science Foundation, etc.), research institutes, particular expeditions, and measurements. Traditionally, the GEBCO data sets and maps contained only bathymetric data on the deepest water areas of the World Ocean (starting from 200 m depth and deeper), which were not presented in the nautical charts in sufficient detail. Today, the major work is being performed on improving the data quality for shallow-water areas. For this purpose, electronic nautical charts (ENCs) collectively prepared by the IHO member countries are used. Many hydrographic services and organizations have already added considerable amounts of bathymetric data on their coastal zones, which led to improvement of the quality of the bottom relief representation in some shallow-water areas. Owing to these data, GEBCO provides the most comprehensive bathymetric model of the entire World Ocean [45].

The modern global model of the land elevation with one-minute resolution can be shown by the ETOPO1 data set. This was compiled on the basis of numerous data from global and regional sources. The distinctive feature of this model is that it has two versions: one displays the ice cover of Antarctica and Greenland (Ice Surface), while the other corresponds to the bedrock beneath ice sheets (Bedrock) [46].

The elevation model based on regional bathymetry sources was developed in the framework of the IBCAO (International Bathymetric Chart of the Arctic

Ocean) and CRM (Coastal Relief Model) projects. The IBCAO was aimed at the creation of the digital data set that contains all of the available bathymetric data north of 64° N for further use in the works that require detailed and precise knowledge of the Arctic Ocean depths and landforms on its bottom. Version 3.0 of the IBCAO data set includes the improved data collected by the arctic countries, the data from accompanying measurements by fishery vessels, and the data obtained by American Navy submarines and research vessels of the other countries [47]. The grid constructed using the modernized gridding algorithm has a resolution of 500 m to distinguish more details on the Arctic Ocean floor, compared to the IBCAO version 1.0 (2.5 km) or 2.0 (2.0 km).

The National Centers for Environmental Information of the National Oceanic and Atmospheric Administration (NCEI NOAA, United States) constructs digital elevation models (DEM) and digital bathymetric models (DBM) with a spatial resolution of three angular seconds for the coastal zones of all of the states, including Alaska. Bathymetric, topographic, and coastal data used in this massif are retrieved from such various sources as federal and local authorities, research organizations, and private companies. This integrated digital model constructed by NCEI for the coastal zone of the United States has provided complete knowledge about the respective areas for the first time by uniting the bathymetry in water areas and the topography of the land. Today, this data set is successfully used for the online tsunami modeling system developed by the Pacific Marine Environmental Laboratory (PMEL) [48].

All these bathymetric data sets are freely accessible and can be used for research and educational purposes. Nevertheless, many countries have their own data on the bottom relief of a higher resolution (one angular second or less), which were obtained from geophysical and engineering surveys in their respective coastal zones. The state and private companies that prospect for and recover oil and gas on the continental shelf possess charts of even more detail. However, these data are usually not available in open access; moreover, in some countries they are even considered confidential, with access being possible on the basis of special contracts and agreements.

3. QUALITY ASSESSMENT OF THE BATHYMETRIC DATA ON THE NORTHEASTERN SAKHALIN SHELF

The bathymetric survey on the shelf and continental slope of northeastern Sakhalin (Figs. 1 and 2a) was carried out in the framework of three international projects: Kurile-Okhotsk Marine Experiment (KOMEX), Hydro-Carbon Hydrate Accumulations in the Okhotsk Sea (CHAOS), and Sakhalin Slope Gas Hydrates (SSGH) [49–51] (hereinafter, we will use KCS abbreviation to refer to these three projects). The obtained data of the measurements were used to construct an 0.5 angular-minute resolution (the step for longitude is $\Delta x \approx 600$ m; the step for latitude is $\Delta y \approx 920$ m) bathymetric chart (Fig. 2b) and for comparison with the chart constructed on the basis of the GEBCO data set (Fig. 2c).

It should be noted that the chart constructed on the basis of the KCS data (Fig. 2b) seems to be more "natural" than the GEBCO-derived chart (Fig. 2c): the former contains a clear boundary of the Sakhalin shelf, and the slope is marked by densely spaced parallel countour lines. The difference between the depths in these two charts differs from –222 to 661 m. The mean square value of the depth difference is 126 m (Fig. 2d), with the average depth within the studied area being approximately 800 m. Such a significant difference in bathymetric data can lead to considerable differences in tsunami heights calculated on the basis of these data. Unfortunately, the bathymetric chart of the studied area, which would be more detailed than the GEBCO chart, was not available to us. Nevertheless, we can attempt to estimate the uncertainties introduced by incomplete knowledge of the bottom topography by comparison of the tsunami wave field obtained from GEBCO data only and that obtained from the GEBCO data with the KCS bathymetric data being added.

4. A NUMERICAL EXPERIMENT TO ESTIMATE THE INFLUENCE OF THE QUALITY OF THE BATHYMETRIC DATA ON TSUNAMI PROPAGATION

It is quite difficult to estimate the influence of errors in the setting of the sea-bottom topography on the results of model computations. There is no commonly accepted technique for such an estimate. In fact, the distortion of the wave field calculated by using inaccurate bathymetric data can be interpreted as an effect of tsunami-wave scattering on bottom irregularities, which were set in the form of a massif with the difference between the depths of the model and the real bottom relief. It is obvious that the influence of scattering is of an integrated ("accumulated") character: the farther the observer is from the source, the more distortion of the wave field occurs. Estimation of the accuracy in the calculation of the maximum tsunami heights near the shore is of principal interest, because it is these values that are usually used in constructing the tsunami zoning maps.

The eastern coast of Sakhalin belongs to the zones of moderate tsunami hazard. According to [52], the expected tsunami height can be up to 1.5 m. It is known [53] that the remote tsunami sources located in the most seismoactive zones of the Pacific are of the highest tsunami hazard for the coasts of the Sea of Okhotsk: despite the definite screening effect of the Kuril Arc, a significant amount of wave energy can

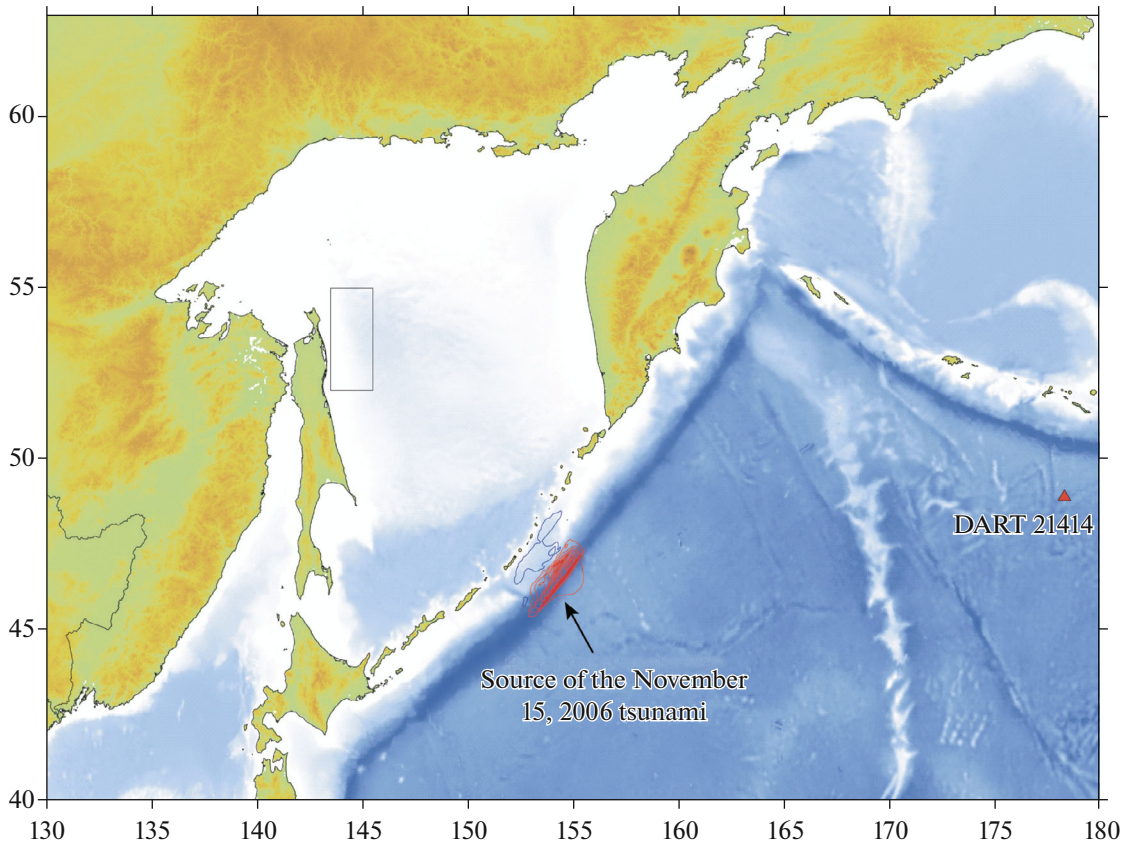

Fig. 1. A bathymetric chart of the northeastern Pacific constructed on the basis of GEBCO_2014 (version 20141103). The rectangle marks the KCS survey area. The red and blue isolines off the coast of the Kuril Islands denote coseismic bottom deformation due to the $M = 8.3$ earthquake of November 15, 2006 (uplift and subsidence, respectively); isolines are drawn with 0.2 m step. The red triangle indicates the location of the DART 21414 deep-water tsunami sensor.

enter the Sea of Okhotsk and cause significant water level variations along the coast of Sakhalin.

In the present research, we will attempt to estimate how the quality of the bathymetric data affects the estimates of maximum tsunami heights on the eastern coast of Sakhalin, with the tsunamigenic $M = 8.3$ earthquake of November 15, 2006, that occurred in the region of Central Kuril Islands as an example. Such a choice is caused by the fact that the parameters of the source of this earthquake are well known from the literature; in addition, it was verified instrumentally that tsunami waves from this event entered the Sea of Okhotsk and reached the coast of Sakhalin [54]. In fact, this gives us grounds to compare the model calculations with the available measurements in order to estimate the differences between tsunami heights calculated with and without KCS bathymetry being taken into account.

A numerical experiment was carried out on a grid of 0.5 angular seconds in resolution and 4801 × 2761 nodes in size, which covers the northwestern Pacific, including the Sea of Okhotsk (Fig. 1). The digital bathymetric data set was compiled on the basis of the GEBCO_2014 data. For calculations, we used a model that is a version of the well known TSUNAMI software for numerical simulation of tsunami wave propagation [6], utilizing the finite-difference approximation of shallow-water linear equations in spherical coordinates [55].

For calculation of the tsunami-source parameters, we used the USGS model [56] to calculate the displacements along the rupture plane within the rectangular area. These displacements were then recalculated into vertical deformations of the sea floor by using the model from [24]. In terms of the shallow-water approximation, which is usually applied for tsunami calculation, the initial deviations of the ocean surface in the source zone completely coincide with sea-floor displacement. However, if the characteristic horizontal scales of coseismic deformations are comparable to the ocean depth, hydrostatic approximation can lead to noticeable errors. In this respect, we used the "non-hydrostatic" solution of the Laplace equation [57] as the initial disturbance on the ocean surface. This is smoothed compared to the bottom deformation. In particular, the maximum deviation of the free surface for the source decreased from 2.7 to 1.9 m [58, 59].

The comparison between the ocean-level variations that were observed and calculated for the loca-

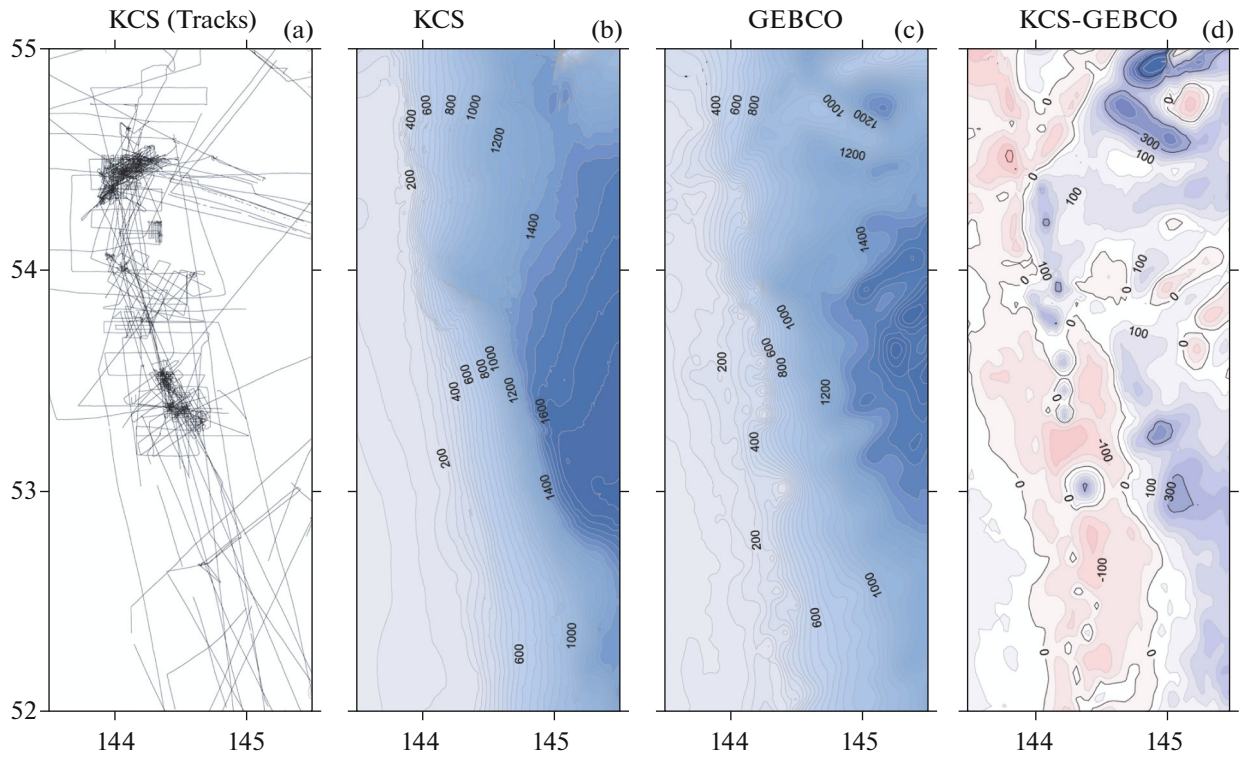

Fig. 2. (a) A map of echosounder tracks in the framework of KCS projects. (b) A map of the bottom topography in the shelf zone and slope of northeastern Sakhalin based on the KCS bathymetric survey. (c) A map of the bottom relief constructed from the GEBCO data. (d) Difference of depths between KCS (Fig. 2b) and GEBCO (Fig. 2c) maps. All depths are in meters.

tion of the DART 21414 deep-water sensor is shown in Fig. 3.

It is seen that arrival of the tsunami wave in the record of the deep-water sensor located at the distance of about 1600 km from the source is noticed 2 hours after the earthquake. The model satisfactorily reproduces both the tsunami wave arrival and the maximum height of the first wave. The sensor is located at a 5375 m depth, approximately 270 km south of Amchitka Island (Aleutian Arc). Such an agreement between the recorded and model waves suggests that the initial conditions that were set in the model of the tsunami source were correct.

In the present work, the estimation of how the bathymetric data quality affects the tsunami-hazard assessment is based on the comparison between the values of the maximum tsunami heights along the northeastern coast of Sakhalin that were obtained by numerical modeling of the November 15, 2006, tsunami using (a) the GEBCO_2014 bathymetric data and (b) with addition of the KCS-derived relief in the rectangular area shown in Fig. 1. In order to estimate the distortion of the tsunami wave field due to different local bathymetry within the studied area off the northeastern coast of Sakhalin, a combined bathymetric grid including the GEBCO_2014 and KCS data was generated. In order to avoid abrupt changes in depth, we interpolated the depth values to provide a smooth transition to the GEBCO bathymetry within the 0.5°-wide band that covers the KCS survey area.

Figure 4 contains the curves of sea-level variations obtained by the wave field calculation for the tsunami of November 15, 2006, for a 5-h time interval at three points on the Sakhalin coast (see Fig. 5) and for two bathymetric models, viz., GEBCO_2014 and the combined GEBCO_2014-KCS. The records of sea-level variations in the southernmost point no. 1 are very similar for both models. The difference becomes noticeable for points nos. 2 and 3, which are located immediately in front of the KCS survey area. The most noticeable difference is observed at point no. 3. It is

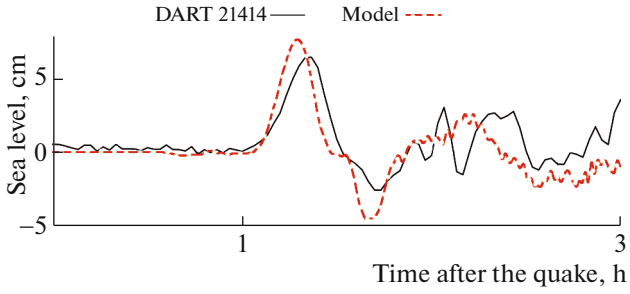

Fig. 3. The records of the real sea-level variations induced by the tsunami of November 15, 2006, at the DART 21414 sensor (black solid curve). The red curve corresponds to the respective model calculations.

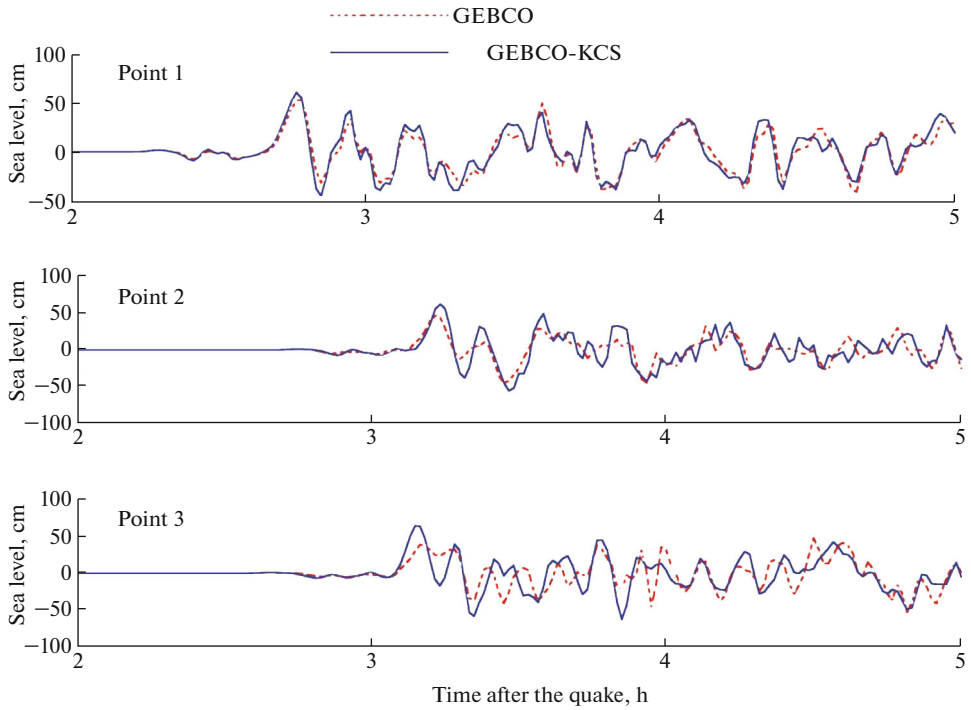

Fig. 4. The records of sea-level variations calculated for three points on the northeastern coast of Sakhalin by the GEBCO_2014 bathymetric data set (red dashed curve) and combined GEBCO-KCS data (blue solid curve).

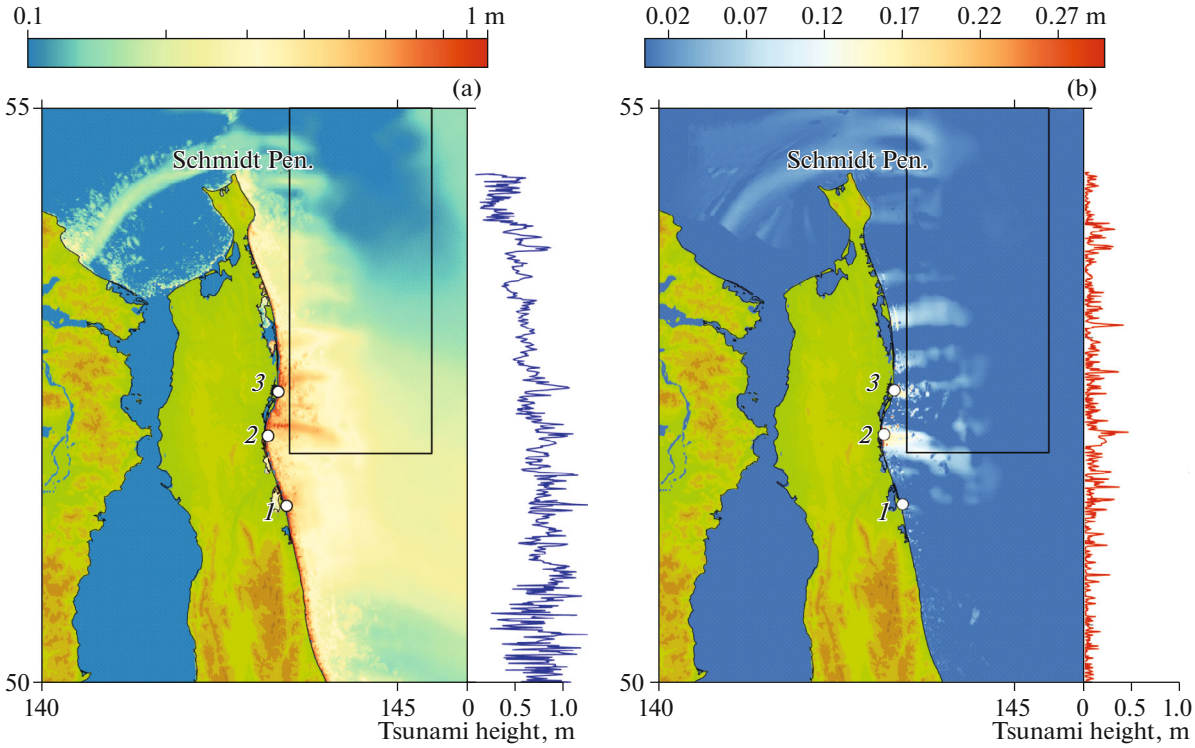

Fig. 5. (a) A map showing the distribution of the maximum tsunami heights on the northeastern coast of Sakhalin, calculated via the GEBCO_2014 bathymetric data set. The solid violet line on the right represents the distribution of maximum tsunami heights along the coast at 10 m depth. (b) A map showing the distribution of the modulus for difference between the tsunami heights obtained by the two models (calculated by the GEBCO_2014 bathymetric data set and combined GEBCO–KCS data) on the northeastern coast of Sakhalin. The solid red line on the right represents the distribution of the modulus of the difference for the maximum tsunami heights along the coast at 10 m depth. The rectangle marks the KCS survey area; the circles mark the positions of the observation points for which the model tidal curves were calculated.

remarkable that the maximum tsunami height in the case of the combined model of bottom topography (GEBCO-KCS) is observed for the first wave, whereas for the GEBCO_2014 model the maximum is noticeable approximately 1.5 h after the arrival of the first wave.

The map of maximum tsunami heights is presented in Fig. 5a. It is clearly seen that the highest tsunami waves are observed on the northeastern coast of Sakhalin. We emphasize that this area is where the objects of the oil-recovery industry are located. In the right part of Fig. 5a, the profile of the tsunami-height distribution along the coast of Sakhalin on 10-m isobath is shown. The characteristic tsunami heights vary between 0.5 and 1 m, with the minimal values being observed on the eastern coast of Schmidt Peninsula.

The map showing the distribution of the modulus for the difference between tsunami heights obtained by the GEBCO and combined bathymetry models is presented in Fig. 5b. In the right part of Fig. 5b, the profile that shows the distribution of the modulus of the height difference along the coast of Sakhalin on a 10-m isobath, as obtained on the mentioned models, is shown. The mean square value of this difference is more than 10 cm for the coast between 51.5 and 54° N and approximately 5 cm for the coast south of this, between 54 and 51.5° N. Remarkably, particular surges occur of up to 0.4 m. In other words, in the area immediately in front of the KCS survey area, the error in the depth setting within the KCS rectangle leads to 15–20% differences in tsunami heights, or even 40–50% at some points.

CONCLUSIONS

Advances in numerical modeling of tsunami propagation in deep water and shelf zones have reached the level where certain research problems become primarily technological and engineering problems. The modern computational capabilities (memory and speed) allow gridded bathymetric data sets to be used in models; the resolutions of these data sets a priori exceed the available bathymetric charts. This is the reason that the quality of the bathymetric data has been the main problem for tsunami research in the recent years. The scope of the present study was limited to estimation of how errors in bathymetry affect the modeling quality for a relatively small area of the Sea of Okhotsk. A 334 × 130 km rectangle covers the northeastern shelf zone and the slope of Sakhalin. The highest errors in the set bathymetry when calculating tsunami heights are observed on the coast between 52 and 54° N. These numerical experiments (under the assumption that the KCS bathymetric data set was close to the true bottom topography) have shown that calculation of tsunami heights on the basis of the GEBCO_2014 data can yield errors of 15–20% (with particular surges of up to 50%).

It must be noted that these conclusions are applicable only to the local conditions related to the quality of bathymetric data in the water area immediately joining the northeastern coast of Sakhalin. It is obvious that errors in setting the bathymetry along the entire path of wave propagation will yield even higher errors.

The results of the present study are the most important in the cases of numerical modeling for tsunami zoning of coasts. Overestimation or underestimation of the maximum tsunami heights in tsunami-hazard assessment may lead to such negative outcomes as excessive expenditures for building coastal infrastructure (in the case of overestimation), human deaths, and economic losses (in the case of underestimation). Development of free accessible high-quality bathymetric data sets is of particular importance for the coastal zones of the Russian Far East, which are the most prone to tsunami effects, viz., Kamchatka, Kuril Islands, Sakhalin, Primorye, and Magadan regions.

ACKNOWLEDGMENTS

This work was supported by the Russian Science Foundation (projects nos. 14-50-00095 and 14-17-00219).

REFERENCES

1. A. B. Rabinovich and M. C. Eblé, Pure Appl. Geophys. **175**, 3281 (2015). doi 10.1007/s00024-015-1058-1
2. F. González, E. Geist, B. Jaffe, U. Kânoğlu, et al., J. Geophys. Res. **114**, C11023 (2009).
3. B. Le Méhauté, *An Introduction to Hydrodynamics and Water Waves* (Springer, 1976).
4. B. W. Levin and M. A. Nosov, *Physics of Tsunamis*, 2nd ed. (Springer, 2016).
5. N. Shuto, in *Tsunami Hazard. A Practical Guide for Tsunami Hazard Reduction*, Ed. by E. N. Bernard (Springer, 1991), p. 171.
6. F. Imamura, in *Long-Wave Runup Models*, Ed. by H. Yeh, P. Liu, and C. Synolakis (World Sci., 1995), p. 43.
7. I. Isozaki and S. Unoki, in *Studies on Oceanography: A Collection of Papers Dedicated to Koji Hidaka* (Tokyo Univ. Press, 1964), p. 389.
8. T. Ueno, Oceanogr. Mag. **17**, 87 (1965).
9. I. Aida, Bull. Earthquake Res. Inst. **47**, 673 (1969).
10. A. Mogi, B. Kawamura, and Y. Iwabuchi, J. Geod. Soc. Jpn. **10**, 180 (1964).
11. T. Hatori, Bull. Earthquake Res. Inst. **43**, 129 (1965).
12. R. Takahasi and T. Hatori, Bull. Earthquake Res. Inst. **40**, 873 (1962).
13. L.-S. Hwang and D. Divoky, J. Geophys. Res. **75**, 6802 (1970).
14. L.-S. Hwang, H. Buttler, and D. Divoky, *Rat Island Tsunami Model: Generation and Open-Sea Characteristics* (U.S. Atomic Energy Commission, 1971).

15. A. S. Alekseev, V. K. Gusiakov, L. B. Chubarov, and Yu. I. Shokin, in *The Study of Tsunamis in the Open Ocean* (Nauka, Moscow, 1978), p. 5.
16. V. K. Gusiakov and L. B. Chubarov, in *The Evolution of Tsunamis from the Source to the Shore* (Radio i Svyaz', Moscow, 1982), p. 16.
17. L. B. Chubarov, Yu. I. Shokin, and V. K. Guisakov, Comput. Fluids **12** (2), 123 (1984).
18. P. L.-F. Liu, C. E. Synolakis, and H. H. Yeh, J. Fluid Mech. **229**, 675 (1991).
19. *Long-Wave Runup Models*, Ed. by H. Yeh, P. Liu, and C. Synolakis (World Sci., 1995).
20. A. Dziewonski, T. Chou, and J. Woodhouse, J. Geophys. Res **86**, 2825 (1981).
21. G. Ekström and M. Nettles, Phys. Earth Planet. Inter. **101**, 219 (1997).
22. I. Aida, J. Phys. Earth **26**, 57 (1978).
23. L. Mansinha and D. Smylie, Bull. Seismol. Soc. Am. **61**, 1433 (1971).
24. Y. Okada, Bull. Seismol. Soc. Am. **75**, 1135 (1985).
25. M. Chinnery, Bull. Seismol. Soc. Am. **51**, 355 (1961).
26. T. Maruyama, Bull. Earthquake Res. Inst. **42**, 289 (1964).
27. F. Press, J. Geophys. Res. **70**, 2395 (1965).
28. J. Savage and L. Hastie, J. Geophys. Res. **71**, 4897 (1966).
29. R. Sato and M. Matsuura, J. Phys. Earth **22**, 213 (1974).
30. V. K. Gusiakov, in *Conditionally Correct Problems of Mathematical Physics in the Interpretation of Geophysical Observations* (Vychisl. Tsentr Sib. Otd. Ross. Akad. Nauk, Novosibirsk, 1978), p. 23.
31. C. Ji, D. J. Wald, and D. V. Helmberger, Bull. Seismol. Soc. Am. **92**, 1192 (2002).
32. C. E. Synolakis and E. N. Bernard, Philos. Trans. R. Soc., A 364, 2231 (2006). doi 10.1098/rsta.2006.1824
33. M. A. Nosov, Izv., Atmos. Ocean. Phys. **50**, 474 (2014).
34. A. V. Bolshakova and M. A. Nosov, Pure Appl. Geophys. **168**, 2023 (2011).
35. M. A. Nosov, A. V. Bolshakova, and S. V. Kolesov, Pure Appl. Geophys. **171**, 3515 (2014).
36. A. V. Bolshakova, M. A. Nosov, and S. V. Kolesov, Moscow Univ. Phys. Bull. **70**, 62 (2015).
37. F. Gonzalez, E. N. Ernard, C. Meinig, M. Eble, et al., Nat. Hazards **35**, 25 (2005).
38. V. V. Titov, F. I. Gonzalez, E. N. Bernard, M. C. Eble, et al., Nat. Hazards **35**, 41 (2005).
39. Y. Wei, E. N. Bernard, L. Tang, R. Weiss, et al., Geophys. Res. Lett. **35**, L04609 (2008).
40. V. V. Titov, in *The Sea*, Vol. 15: *Tsunamis*, Ed. by E. N. Bernard and A. R. Robinson (Harvard Univ. Press, 2009), p. 371.
41. NOAA National Centers for Environmental Information, ETOPO5 5-minute gridded elevation data. http://www.ngdc.noaa.gov/mgg/global/etopo5.HTML.
42. M. T. Jones, A. R. Tabor, and P. Weatherall, *GEBCO Digital Atlas: CD-ROM and Supporting Volume* (British Oceanographic Data Center, Birkenhead, 1994).
43. W. H. F. Smith and D. Sandwell, Science **227**, 1956 (1997).
44. General Bathymetric Chart of the Oceans, GEBCO one minute grid. http://www.gebco.net/data_and_products/gridded_bathymetry_data/gebco_one_minute_grid.
45. British Oceanographic Data Centre, The GEBCO_2014 grid. http://www.bodc.ac.uk/data/documents/nodb/301801/.
46. C. Amante and B. W. Eakins, *ETOPO1 1 Arc-Minute Global Relief Model: Procedures, Data Sources and Analysis* (National Geophysical Data Center, Boulder, 2009). http://www.ngdc.noaa.gov/mgg/global/relief/ETOPO1/docs/ETOPO1.pdf.
47. M. Jakobsson, L. Mayer, B. Coakley, et al., Geophys. Res. Lett. **39**, L12609 (2012). http://www.ngdc.noaa.gov/mgg/bathymetry/arctic/2012GL052219.pdf.
48. NOAA National Centers for Environmental Information, U.S. coastal relief model. http://www.ngdc.noaa.gov/mgg/coastal/crm.html.
49. *Hydro-Carbon Hydrate Accumulations in the Okhotsk Sea (CHAOS Project Leg I and Leg II)*, Ed. by T. Matveeva, V. Soloviev, H. Shoji, and A. Obzhirov (VNII-Okeangeologia, St. Petersburg, 2005).
50. *Operation Report of Sakhalin Slope Gas Hydrate Project 2011*, Ed. by H. Shoji, Y. K. Jin, A. Obzhirov, and B. Baranov (Kitami Inst. of Technology, Kitami, 2012).
51. *KOMEX II, Kurile Okhotsk Sea Marine Experiment: Cruise report RV Akademik M. A. Lavrentyev cruise 29, Leg 1 and Leg 2: Vladivostok - Pusan - Okhotsk Sea - Pusan - Okhotsk Sea - Pusan - Vladivostok*, Ed. by N. Biebow, R. Kulinich, and B. Baranov (GEOMAR, Kiel, 2003).
52. G. V. Shevchenko, A. V. Fain, A. B. Rabinovich, and R. N. Mansurov, in *Natural Disasters and Hazards in the Russian Far East* (Dal'nevost. Otd. Akad. Nauk SSSR, Vladivostok, 1990), **Vol. 1**, p. 253.
53. V. K. Gusiakov, L. B. Chubarov, and S. A. Beisel, J. Volcanol. Seismol. **9**, 276 (2015).
54. L. I. Lobkovskii, E. A. Kulikov, A. B. Rabinovich, A. I. Ivashchenko, I. V. Fain, and T. N. Ivel'skaya, Dokl. Earth Sci. **419**, 320 (2008). doi 10.1134/S1028334X0802030X
55. I. V. Fine, E. A. Kulikov, and J. Y. Cherniawsky, Pure Appl. Geophys. **170**, 1295 (2013).
56. G. Hayes, "Preliminary finite fault results for the Nov 15, 2006 Mw 8.3 Kuril Islands earthquake (version 1)." http://earthquake.usgs.gov/earthquakes/eventpage/usp000exfn#finite-fault.
57. I. V. Fain and E. A. Kulikov, Vychisl. Tekhnol. **16** (2), 111 (2011).
58. M. A. Nosov and S. V. Kolesov, Moscow Univ. Phys. Bull. **64**, 208 (2009).
59. M. A. Nosov and S. V. Kolesov, Pure Appl. Geophys. **168**, 1223 (2011).

Translated by N. Astafiev